International Journal on
"Technical and Physical Problems of Engineering"
(IJTPE)
Published by International Organization of IOTPE

ISSN 2077-3528
IJTPE Journal
www.iotpe.com
ijtpe@iotpe.com

September 2021 | Issue 48 | Volume 13 | Number 3 | Pages 25-34

WORKSPACE OF A HEXAPOD

M. Atify [1] M. Bennani [2] A. Abouabdellah [1]

1. Laboratory of Engineering Science (LSI) ENSA, Ibn Tofail University, Kenitra, Morocco, atifym@gmail.com, a.abouabdellah2013@gmail.com
2. Laboratory of Mechanics and Industrial Processes and Process (LM2PI), ENSAM, Mohamed V University, Rabat, Morocco, m.bennani@um5s.net.ma

Abstract- During the movement of a robot its center of mass reaches several positions in space, it is the workspace, our objective is to determine the parameters that influence the increase and decrease of this workspace in order to optimize the robot's performance. In this article, the study carried out concerns the workspace of a hexapod robot whose legs are arranged linearly while keeping the robot's body horizontally. Simulations of the workspace are programmed by an algorithm on Visual basic of the SolidWorks software, Also the simulations of the workspace are made, in a horizontal plane located at a well determined height. A graphic interface makes it possible to introduce the different dimensions of the legs and the different contact distances between the legs and the ground. The simulated results are validated experimentally on a robot made in the laboratory.

Keywords: Workspace, Hexapod, GUI, SolidWorks Algorithm, Geometry.

1. INTRODUCTION

There are two types of walking robots, wheeled robots which have among the advantages the speed of displacement [1, 2] and legged robots. These are slower than wheeled robots but they have an advantage in addition to their stability, the moving on rugged terrain [3, 4, 5, 6]. The hexapod robot studied in our article belongs to category of walking robots with 6 legs.

Several works have been developed for serial and parallel robots concerning many fields [7, 5, 8] (Kinematics, dynamics, workspace). The [9], [10] and [11] used in their studies the geometric study of serial robots. However, they are few works treating the workspace of the legged robots due to their complexity [12, 13, 14].

The [15] and [16] used the direct and inverse kinematics to define a specific point position of a robot in which the legs are distributed symmetrically around the platform.

The resolution of complex issues is done through the use of numerical methods such as [17] that used Matlab to determine the hot spot and lifetime of the transformer. The [18] used SolidWorks for a simulation and optimization design of sorting tables before they are manufactured, a numerical modeling by [19] is carried out according finite elements to predict the mechanical characteristics of bio-loaded PVC.

Softwares are widely used for simulating the legged robots such as [20] which used Python software. [21]used the Matlab software to determine the angles, the torques in each joint for a given trajectory of an hexapod robot.

Some studies are achieved concerning the robot's workspace. [22] and [23] have been interested in the workspace of parallel manipulator robots of the Stewart type. The kinematic method was applied to optimize the workspace for parallel manipulators [24]. The [25] has treated the workspace of 2-RPR planar parallel mechanisms. [26] has analyzed the workspace of a 3 PPPS parallel robot. In [8] is established the workspace of the foot end of a robot based on the kinematic of the robot. The [27] has considered the workspace of a radial symmetrical robot by the combination of three planar parallel mechanisms. The [28] has treated the displacement of a point of a leg connected by 2 DOF of a quadruple.

Our study focuses on the determination of the workspace of the hexapod robot presented in section 2. In section 3 the workspace of a leg is developed, while section 4 dealt with the workspace of the hexapod. In section 5 a graphical interface is used and a program on SolidWorks is developed to simulate the hexapod robot Workspace. In section 6, many of the experiments are achieved with the hexapod robot. Section 7 is concerning with the analysis of the established results and finally, a conclusion is presented in the last section.

2. ROBOT PRESENTATION

The used hexapod robot is composed of 6 legs arranged as shown in Figure 1, each leg as shown in Figure 2, is composed of 3 parts: thigh, tibia, and foot.

The body of the robot (the platform) is linked by joints with all the legs at points D_i, i = 1,…,6. The thigh of the leg is in a revolute connection with the tibia at point C. The tibia is in a revolute connection with respect to foot at point B. At point A the contact between the leg and the ground is achieved.

The movements of the different parts of the robot's legs are actuated by servo motors. The legs are in contact

with the ground, at a distance L along the $\vec{x}$ axis, and a distance d along the $\vec{y}$ axis as shown in Figure 1.

The workspace is the set of positions that can be reached by the Center of Mass (COM) of the Robot's body during its motion. The robot in our case is considered supporting a load that must remain horizontal with no tilt. This is one major constraint taken in our study.

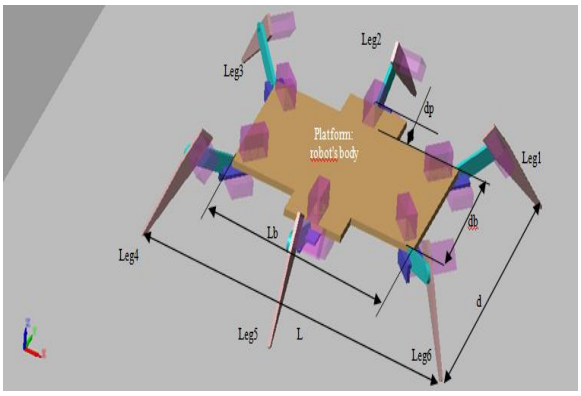

Figure 1. Global structure of hexapod robot [21]

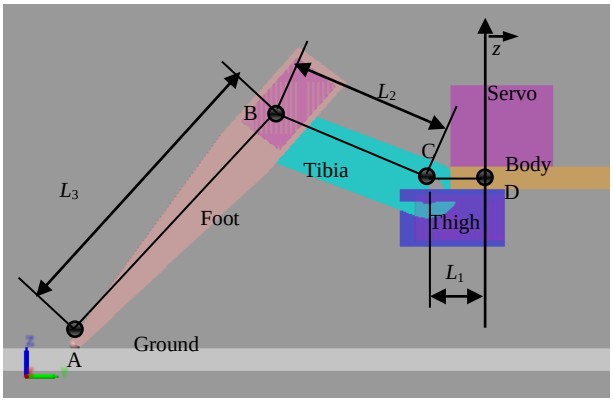

Figure 2. Description of a leg [21]

3. LEG WORKSPACE

3.1. Modeling

At point A in Figure 3, the contact between the foot (L_3), and the ground at point A allows three rotations. One of them is carried out around the body itself. So the movement of the foot (L_3) is modeled by two rotations angles around point A [16], [29], [30], the ψ and O_3 which are defined in spherical coordinates as follows.

The angle ψ is defined around the $\vec{z}$ axis with $\vec{z} = \vec{z}_4$. The corresponding rotation matrix is:

$$H_{04} = \begin{pmatrix} \cos\psi & -\sin\psi & 0 \\ \sin\psi & \cos\psi & 0 \\ 0 & 0 & 1 \end{pmatrix} \quad (1)$$

The second angle O_3 is around the $\vec{y}_4$ axis with $\vec{y}_4 = \vec{y}_3$. So the rotation matrix is given by:

$$H_{43} = \begin{pmatrix} \cos O_3 & 0 & \sin O_3 \\ 0 & 1 & 0 \\ -\sin O_3 & 0 & \cos O_3 \end{pmatrix} \quad (2)$$

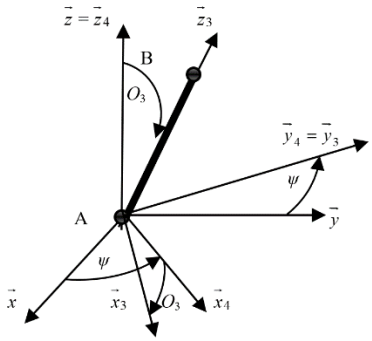

Figure 3. Representation of the foot movement (L_3) relative to ground

At point B in Figure 4, the link (L_2) performs a rotational movement with respect to the foot (L_3). The rotation angle O_2 is around the axis $\vec{y}_3$ and its rotation matrix is:

$$H_{32} = \begin{pmatrix} \cos O_2 & 0 & \sin O_2 \\ 0 & 1 & 0 \\ -\sin O_2 & 0 & \cos O_2 \end{pmatrix} \quad (3)$$

The workspace of point B is a hollow hemisphere of radius the length of the Tibia (L_3).

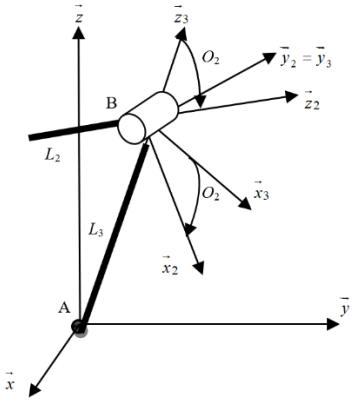

Figure 4. Representation of the movement of Tibia (L_2) compared to the foot (L_3)

At point C in Figure 5, the link L_1 performs with respect to the tibia L_2 a rotational movement defined by the angle O_1, around the axis $\vec{y}_2$

The associated rotation matrix is:

$$H_{21} = \begin{pmatrix} \cos O_1 & 0 & \sin O_1 \\ 0 & 1 & 0 \\ -\sin O_1 & 0 & \cos O_1 \end{pmatrix} \quad (4)$$

The workspace of point C is a spherical volume with maximum radius L_3+L_2 and minimum radius L_3–L_2. This minimum radius leads to a constraint in the Workspace since we can't reach the points which are located inside the sphere of minimum radius.

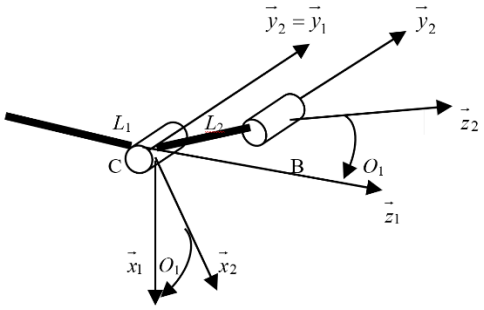

Figure 5. Representation of the movement of the thigh (L_1) in relation to the Tibia (L_2)

At the point D, the platform (Body) of the robot performs with respect to the link (L_1), a rotational movement defined by an angle *Ob* (rotation of Body) around the axis $\vec{x}_1$.

The rotation matrix is:

$$H_{1b} = \begin{pmatrix} 1 & 0 & 0 \\ 0 & \cos O_b & -\sin O_b \\ 0 & \sin O_b & \cos O_b \end{pmatrix} \quad (5)$$

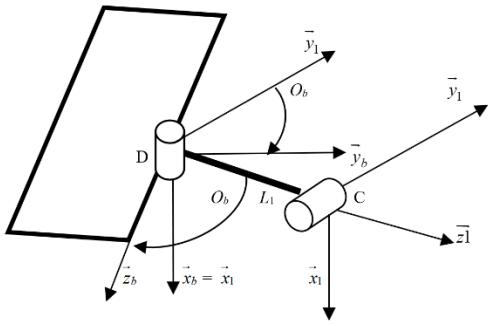

Figure 6. Representation of the movement of the Robot's platform with respect to Thigh (L_1)

In the study, the robot's platform remains horizontal during the movement, since in D the rotation of the link (L_1) is around the axis perpendicular to the platform. So, the Thigh (L_1) also moves in the horizontal plane and can only translate in a horizontal plane and rotate around the vertical axis.

3.2. WorkPlane of the Point D in the Plane (*x*, *z*)

The point D is located with respect to the ground by the vector $\overrightarrow{AD}$ which can be expressed as:

$$\overrightarrow{AD} = \overrightarrow{AB} + \overrightarrow{BC} + \overrightarrow{CD} = L_3 \cdot \vec{z}_3 - L_2 \cdot \vec{z}_2 - L_1 \cdot \vec{z}_1 \quad (6)$$

The projection on $(A, \vec{x})$ line gives:

$$X_d = L_3.\cos(O_3) + L_2.\cos(O_2 + O_3) + \varepsilon.L_1 \quad (7)$$

with the limit positions are defined by ε=1 and ε = -1.

The projection on $(A, \vec{z})$ line yields to

$$Z_d = L_3.\sin(O_3) + L_2.\sin(O_2 + O_3) \quad (8)$$

The trajectory of point D is obtained by a Python program in Figure 7.

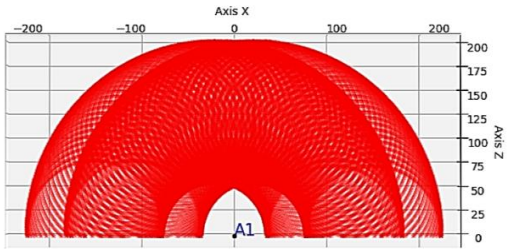

Figure 7. WorkPlane of point D in vertical plane (*x*, *z*) programmed with Python

3.3. Workspace of the Point D

The workspace of the point D is obtained by rotating the WorkPlane around vertical axis as shown in Figure 8.

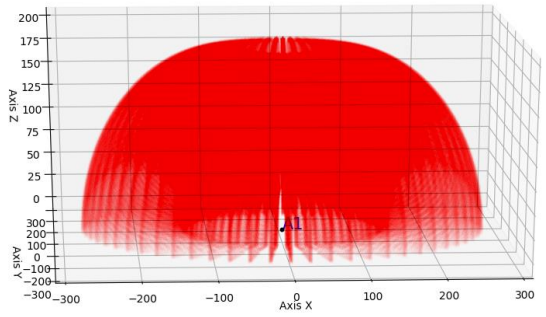

Figure 8. Workspace of point D programmed in Python

4. THE ROBOT'S BODY WORKSPACE

The robot's workspace is determined, from the workspace of a leg, by extending it overall 6 legs. The dimensions of the robot's body and the contact distances with the ground are well respected.

4.1. Geometric Study of the Workspace

In our study, a geometric approach is used to determine the workspace of the hexapod robot. At the start, the highest reached position by the robot is finding. The COM of the robot will be located at a maximum height noted *h* ($h = Z_{max}$). After the Robot's platform is moved slightly downwards. Therefore, the set of reached positions by the COM is called WorkPlane.

To keep the robot's platform in a horizontal plane we have to move it by the translations along $\vec{x}$ and $\vec{y}$ axes and the rotation around the vertical axis $\vec{z}$.

The Robot's platform is lowered vertically to another height. Then the same process is repeated to determine the WorkPlane in this new plane. Thus the same step is repeated until the Robot's body reaches the minimum position. Finally, the set of these WorkPlanes gives the Workspace of the robot.

4.1.1. Maximum Position of the Robot

Since the orientation configurations of all the legs are identical, their lengths are equals and symmetrical with respect to the $\vec{x}$ and $\vec{y}$ axes. The maximum position height of the robot corresponds to a position of point G on the vertical noted Gmax of height *h*. It is a position

obtained when the tibia and the foot are aligned with respect to the L_2+L_3 length as shown in Figure 9.

The geometric calculation using the distances between the points A, B, C, D and K gives the following relations:

$$R_{po} = L_1 + \sqrt{((L_2 + L_3)^2 - Z_{\max}{}^2)} \quad (9)$$

with *Rpo* is the initial plane radius.

$$Rpo = \sqrt{(L_2 + L_3)^2 - h^2} + L_1 = \sqrt{\left(\frac{L - L_b}{2}\right)^2 + \left(\frac{d - d_b}{2}\right)^2} \quad (10)$$

We find the maximum height $Z_{\max}$ as:

$$Z_{\max} = \sqrt{((L_2 + L_3)^2 - (\sqrt{\left(\frac{L - L_b}{2}\right)^2 + \left(\frac{d - d_b}{2}\right)^2} - L_1)^2)} \quad (11)$$

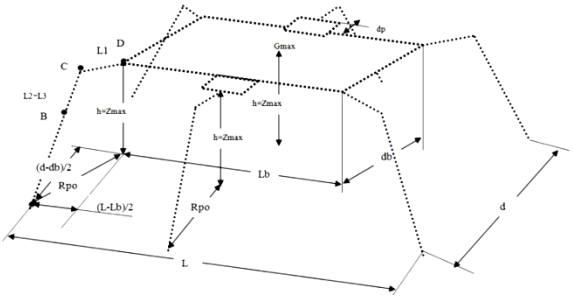

Figure 9. The maximum height of the robot

4.1.2. Minimum Position of the Robot

In this case, the robot's body, always maintained in a horizontal plane, is lowered vertically to reach the low position called $Z_{\min}$. The condition is necessary between the contact distances and the dimensions of the legs, to ensure a contact is:

L_3+L_2+L_1 must be greater than Rpo, given by Equation (10). This a mean to check the configuration functionality.

So, we can write:

$$L_3 + L_2 + L_1 \geq \sqrt{\left(\frac{L - L_b}{2}\right)^2 + \left(\frac{d - d_b}{2}\right)^2} \quad (12)$$

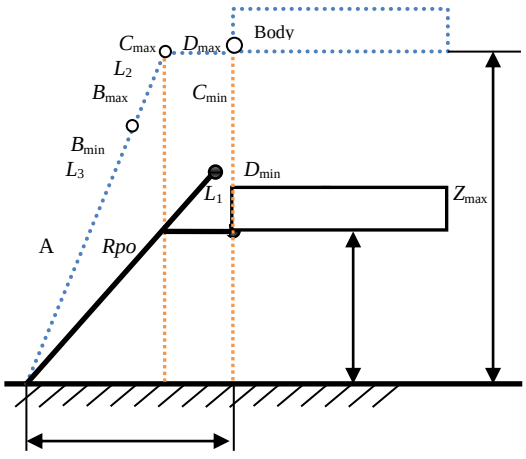

Figure 10. Representation, in black of the minimum robot's position $Z_{\min}$, and the maximum position in dotted blue $Z_{\max}$

The minimum height $Z_{\min}$ is determined geometrically by:

$$Z_{\min} = \sqrt{((L_3 - L_2)^2 - (\sqrt{\left(\frac{L - L_b}{2}\right)^2 + \left(\frac{d - d_b}{2}\right)^2} - L_1)^2)} \quad (13)$$

If the following condition is ensured

$$L_3 - L_2 \leq \sqrt{\left(\frac{L - L_b}{2}\right)^2 + \left(\frac{d - d_b}{2}\right)^2} - L_1 \quad (14)$$

Then the robot can reach the ground with $Z_{\min}$=0.

4.1.3. Intermediary Position of the Robot

The robot's platform is lowered vertically by a distance *h–Z*. In this plane of height *Z*, the displacement of the point G is limited by the dimensions of the legs.

If we consider a displacement of the robot's body in the positive quadrant of $\vec{x}$ and $\vec{y}$, the movement will be limited by the length of the leg 4. This will stretch it to its maximum (L_2+L_3) while the other legs will shrink. So, the limit will be imposed by the leg four.

By the same reasoning, the movement of the robot's body in the positive quadrant of $\vec{x}$ and negative of $\vec{y}$ is limited by the length of the leg three.

Similarly, the displacement of the robot's body in the negative quadrant of $\vec{x}$ and negative of $\vec{y}$ is limited by the length of the leg one.

Also, the movement of the robot's body in the negative quadrant of $\vec{x}$ and positive of $\vec{y}$ is limited by the length of the leg six.

Since legs two and five are placed between the other legs, they will not reach their maximum length.

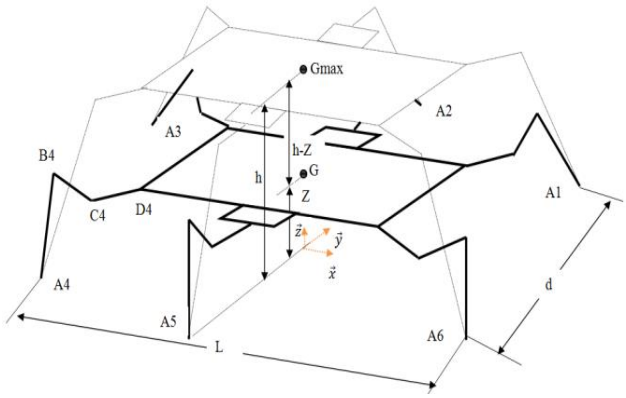

Figure 11. Maximum position in dotted lines, and an arbitrary position at a height *Z* in solid line

4.1.4. COM Displacements in the Horizontal Plane of Height *Z*

Considering the positive quadrant on the $\vec{x}$ axis and the $\vec{y}$ axis, we are looking for all the reached positions of the point D_4 (Figure 12).

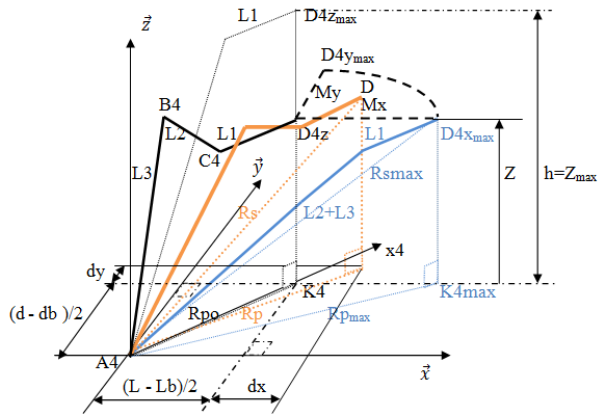

Figure 12. Displacement of the point D in a horizontal plane of height Z
Representation of the position of point D at the desired height Z
Position of point D in any position in the plane of height Z
Maximum position of point D on the x axis, obtained for L_2+L_3

For any height Z, the maximum plane radius is:

$$R_{p\max} = \sqrt{(L_2 + L_3)^2 - Z^2)} + L_1 \quad (15)$$

The spherical radius is determined as:

$$R_s = \sqrt{(R_p^2 + Z^2)} \quad (16)$$

So, we can establish the maximum spherical radius as:

$$R_{s\max} = \sqrt{(R_{p\max}{}^2 + Z^2)} \quad (17)$$

We thus get the maximum displacement of D_4 along the $\vec{x}$ axis:

$$M_x = \sqrt{R_{p\max}^2 - \left(\frac{d-d_b}{2}\right)^2} - \left(\frac{L-L_b}{2}\right) \quad (18)$$

$$M_x = \sqrt{(\sqrt{(L_2+L_3)^2 - Z^2} + L_1)^2 - \left(\frac{d-d_b}{2}\right)^2} - \left(\frac{L-L_b}{2}\right) \quad (19)$$

The maximum trajectory in the plane of height Z is described by a circle. The center is the point A_4 and the radius is R_s. The radius R_{pmax} represents the projection of the spherical radius R_s in the plane of height Z by the following equations:

$$\left(dx + \frac{L-L_b}{2}\right)^2 + \left(dy + \frac{d-d_b}{2}\right)^2 = R_{pmax}{}^2 \quad (20)$$

$$dy = \sqrt{R_{pmax}{}^2 - \left(dx + \frac{L-L_b}{2}\right)^2} - \left(\frac{d-d_b}{2}\right) \quad (21)$$

Let "My" be the maximum displacement of D_4 along the $\vec{y}$ axis given for dx=0. So, we can express it as:

$$M_y = \sqrt{R_{p\max}^2 - \left(\frac{L-L_b}{2}\right)^2} - \left(\frac{d-d_b}{2}\right) \quad (22)$$

$$M_y = \sqrt{(\sqrt{(L_2+L_3)^2 - Z^2} + L_1)^2 - \left(\frac{L-L_b}{2}\right)^2} - \left(\frac{d-d_b}{2}\right) \quad (23)$$

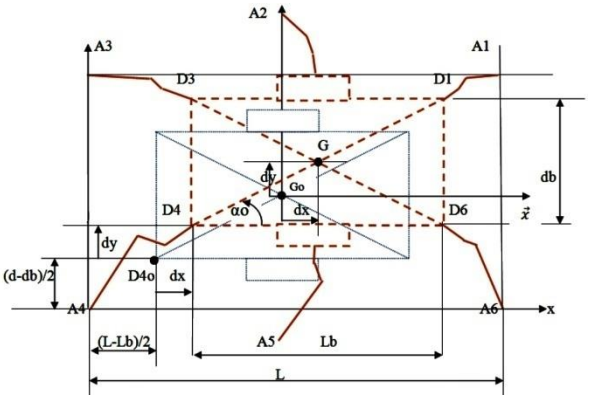

Figure 13. Top view of the displacement of points D and G the Initial position in blue and displacement of distances (dx, dy) in brown

When the point D_4 moves from the initial position D_{4o} to a position D_4 by a distance dx along the $\vec{x}$ axis and dy along the $\vec{y}$ axis, then G moves from its initial position Go to a position G by the same distance as point D_4. Knowing that dx varies from 0 to M_x.

4.1.5. COM Positions due to Rotations around the Vertical Axis $\vec{z}$

In a plane of a known height Z, let us now consider a rotation of the robot's platform around point D_4 located at a distance dx along $\vec{x}$ and dy along $\vec{y}$ with respect to the initial position D_{4o}.

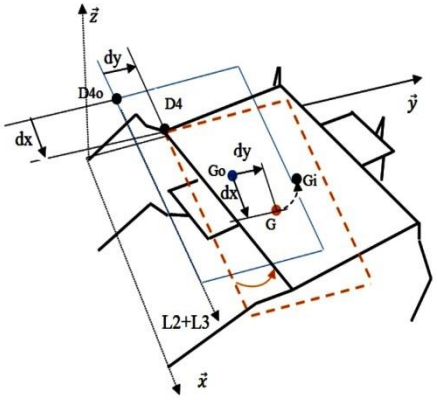

Figure 14. View in space of the positions of point G, for a rotation around D_4, in blue the initial position, in brown the displacement of distances (dx, dy), in black the rotation of the Robot's body around D_4

By the rotation around point D_4 which is caused by the lengthening of the leg 6, the point G is on an arc of a circle. Its center is the point D_4 and the radius is the diagonal of the platform of the robot. Thus, the position of G is identified by an angle which varies from α_0 up to α_{max}.

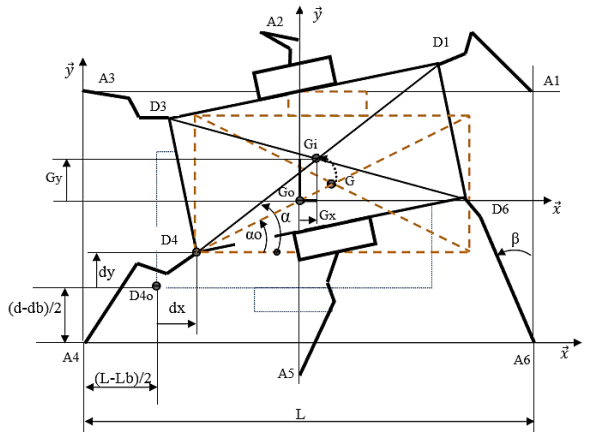

Figure 15. Top view of the positions of point G, for a rotation around D_4, in blue the initial position, in brown the displacement of distances (dx, dy), in black the rotation of the Robot's body around D_4

The angle α_0 is given by:

$$\alpha_0 = \text{arctg}\left(d_b / L_b\right) \tag{24}$$

The coordinates G_x and G_y of the point G during the movement are established as:

$$G_x = dx - \frac{L_b}{2} + \left(\frac{\sqrt{{d_b}^2 + {L_b}^2}}{2}\right)\cos(\alpha) \tag{25}$$

$$G_y = dy - \frac{d_b}{2} + \left(\frac{\sqrt{{d_b}^2 + {L_b}^2}}{2}\right)\sin(\alpha) \tag{26}$$

We look for the angle of rotation α, by projecting the distances between the points A_4, D_4, A_6 and D_6, on the axes $\vec{x}$ and $\vec{y}$ as follows:

Projection/ $\vec{x}$:

$$\left(L - dx - \frac{L - L_b}{2}\right) = R_p \sin(\beta) + L_b \cos(\alpha) \tag{27}$$

Projection/ $\vec{y}$:

$$\left(d + dy - \frac{d - d_b}{2}\right) + L_b \sin(\alpha) = R_p \cos(\beta) \tag{28}$$

where α is maximum (α_{max}) when the radius R_p is maximum (R_{pmax}). It's obtained when the leg 6 is at its maximum length for L_2 and L_3 which are aligned. By eliminating β between Equations (27), (28) and (15) we obtain, by arranging this equations:

$$2L_b\left(\left(\frac{L - L_b}{2} - dx\right)\cos(\alpha_{max}) - \left(\frac{d + d_b}{2} + dy\right)\sin(\alpha_{max})\right) = \left(\frac{L - L_b}{2} - dx\right)^2 + {L_b}^2 + \left(\frac{d + d_b}{2} + dy\right)^2 - \left(\sqrt{(L_2 + L_3)^2 - Z^2} + L_1\right)^2 \tag{29}$$

For the resolution of this equation, one poses:

$$AA = \frac{L + L_b}{2} - dx \tag{30}$$

$$BB = \frac{d + d_b}{2} + dy \tag{31}$$

$$CC = \frac{AA^2 + Lb^2 + BB^2 - \left(\sqrt{(L_2 + L_3)^2 - Z^2} + L_1\right)^2}{2L_b} \tag{32}$$

$$EE = \sqrt{(AA^2 + BB^2)} \tag{33}$$

Thus, we obtain the following relationship

$$\alpha_{max} = \arccos\left(CC / EE\right) - \arccos\left(AA / EE\right) \tag{34}$$

After this calculation, the approach used to determine workspace in case of rotation can be formulated as follows:

For a given height Z, M_x, and M_y are calculated. Then, for a point D_4 located at any distance (dx, dy) from initial position D_{40} (dx varies from 0 to M_x) we look for αmax. This is the maximum angle reached by G. Then all the positions of point G (G_x, G_y) are determined with α varies from α_0 to α_{max}. In the end, these positions of G could be drawn as shown in the following Figure 16 corresponding to a program established in SolidWorks Software.

In the same way, the calculation is used for a rotation around the points D_1, D_3, and D_6, to find the workspace of the robot due to the rotations of the body.

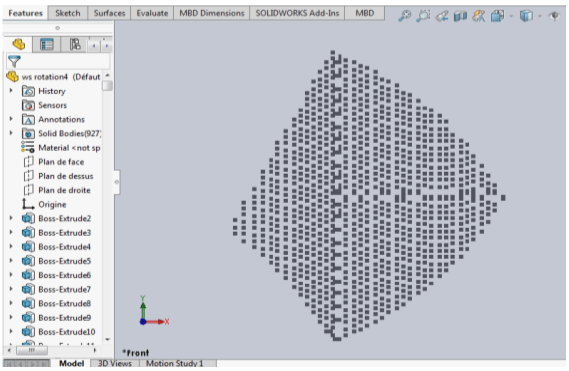

Figure 16. WorkPlane with SolidWorks of the COM for a rotation around the point D_4

5. SIMULATION ON SOLIDWORKS

5.1. Presentation of the Graphical User Interface

A program is built on SolidWorks which allows determining workspace of a hexapod robot. The necessary information is introduced on the first page of the GUI, in Figure 17. On the second page in Figure 18, the type simulation is chosen to simulate the workspace either in space or in a plane located at a height Z. Then the result of the simulation is displayed on a SolidWorks window.

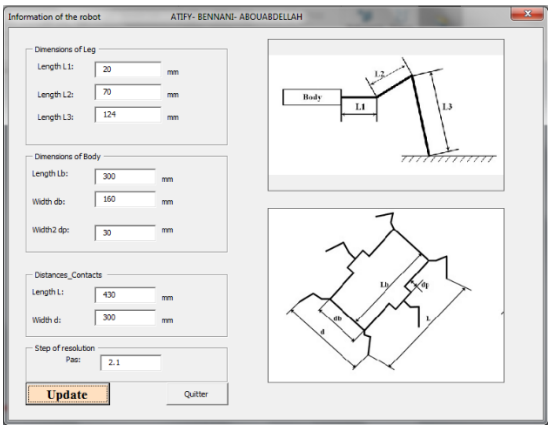

Figure 17. First GUI page to introduce information about the robot

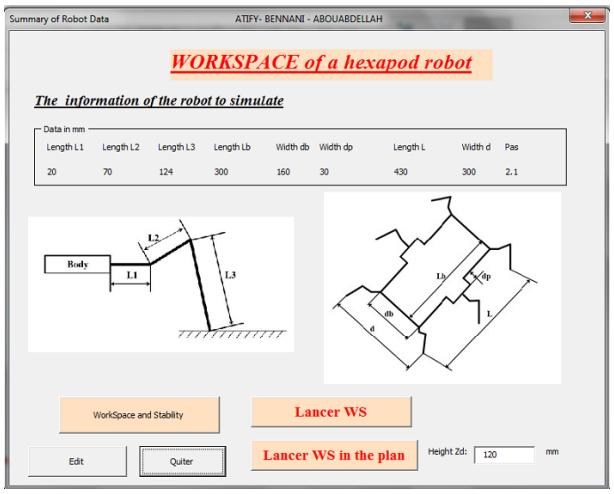

Figure 18. Second GUI page to check the robot information and launch the workspace simulation

5.2. Robot's Workspace

In this example, the necessary dimensions used are: L_1=20mm, L_2=70mm, L_3=124mm, L=430mm, d=300mm, L_b=300mm, d_b=160mm, d_p=30mm

Figure 19 shows an example of a workspace established in the SolidWorks software by introducing the dimensions in the GUI interface. The spherical geometries are removed due to the workspace limit of the point C (limitation between L_3+L_2 and L_3–L_2 for each leg).

From this result, the maximum height that the robot can reach is known for this configuration. The maximum height is h=179mm. For each height, the different limit positions will be known, in particular the maximum position along the $\vec{x}$ axis and the maximum position along the $\vec{y}$ axis. Also for a given height, we can check whether the robot will reach some positions.

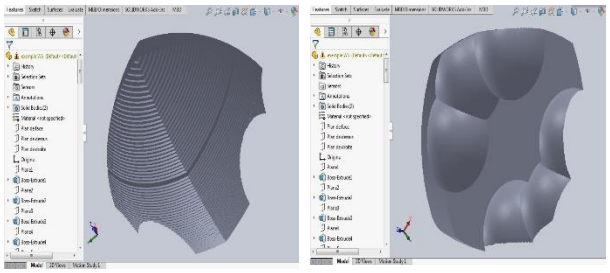

(a) (b)

Figure 19. Workspace in space, (a) profile view in perspective, (b) view from behind in perspective

5.2.1. WorkPlane in a Horizontal Plane (x, y)

The WorkPlane of the COM displacement of the Robot's platform is obtained with a plane section moved in the SolidWorks workspace. It acts up to the desired horizontal height plane shown in blue in Figure 20.

From these results, the WorkPlanes shown in blue are determined for each height. The different limit positions will be known, in particular the maximum position along the $\vec{x}$ axis and the maximum position along the $\vec{y}$ axis. Also for a given height, we can check if the robot will reach some positions like the case of Figure 20b.

In these examples, the WorkPlanes are determined respectively, for the height Z=120mm in Figure 20a. the height Z=46mm in Figure 20b.

For the height Z=120mm as an example, the displacement maximal along $\vec{x}$ axis is 93.4mm while the maximal displacement along $\vec{y}$ axes is 89.7mm.

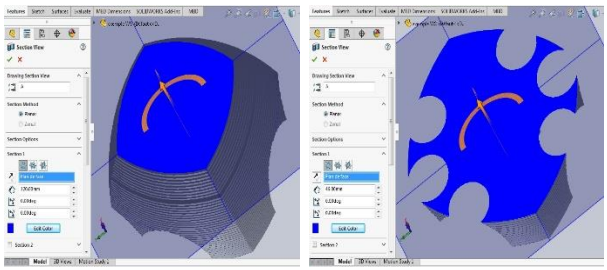

(a) (b)

Figure 20. The result of the simulation of the workspace in horizontal planes which are located at given heights, (a) WorkPlane for height Z=120mm, (b) WorkPlane for height Z=46mm

5.2.2. WorkPlane: Displacement in a Vertical Plane (z, x)

The WorkPlane of the displacement of the COM of the Robot's platform in a vertical plane for a distance y, this WorkPlane is obtained with a section plane moved in the workspace found by SolidWorks, up to the desired distance plane shown in pink in Figure 21.

From these results, the WorkPlane shown in pink is determined for each vertical plane located at a distance y from the initial position. The different limit positions will be known, in particular the maximum position along the $\vec{x}$ axis for a height Z.

In these examples, the WorPlanes are determined respectively, for a distance y=70mm in Figure 21a, a distance y=100mm in Figure 21b.

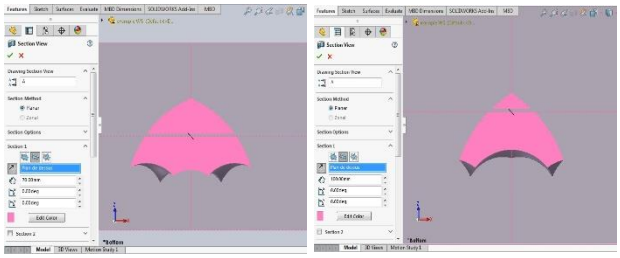

(a) (b)

Figure 21. Result of the workspace in vertical planes located at given distances along the $\vec{y}$ axis, (a) WorkPlane in the vertical plane for y=70mm, (b) WorkPlane in the vertical plane for y=100mm

6. EXPERIMENTATION

6.1. Data Used

The design of the hexapod robot is dealing with the following dimensions:

L_b=300mm, d_b=160mm, d_p=30mm, L_1=20mm, L_2=70mm, L_3=124mm

The distances of contacts are fixed as:
L=430mm (between A_1 and A_3) and d=300mm (between A_1 and A_6) as shown in Figure 22.

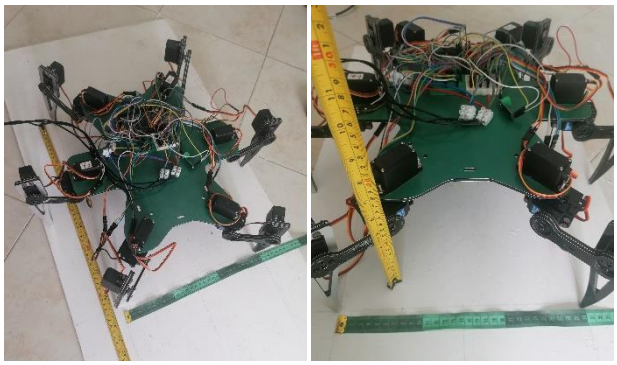

(a) (b)

Figure 22. Contact distances between the robot's legs and the ground, (a) top view (b) perspective view

6.2. Measurements

The robot is placed to respect the contact distances with the ground. Then the desired manipulations are carried out as:

- Position the robot in the maximum position, to determine the maximum height h.
- Position the robot at any height Z to determine the maximum positions along the x and y axes in this plane.
- Rotate the Robot's body around the vertical axis to determine the reached positions by the robot.

In our case, depending on the dimensions given previously, the maximum measured height of the Robot's platform in Figure 23a is h=177mm.

An experiment is made for a height Z=120mm. It gives:

-The maximum position along the $\vec{x}$ axis is: 91mm, as shown in Figure 23b.

- The maximum position along the $\vec{y}$ axis is: 88mm, as shown in Figure 23c.

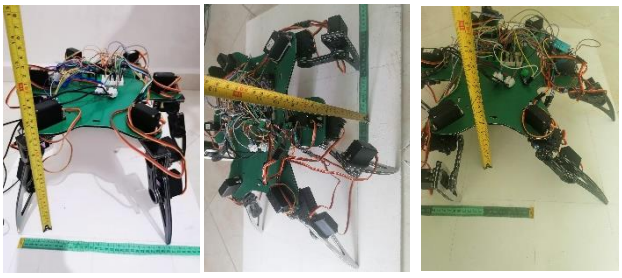

(a) (b) (c)

Figure 23. (a) Robot in the maximum height position, (b) the maximum displacement measured along the $\vec{x}$ axis, (c) the maximum displacement measured along the $\vec{y}$ axis, these displacements for the height Z=120mm

7. RESULTS ANALYSIS

We notice that the measured displacements are almost the values given by simulation. Some differences due to the technological solutions of the joints present clearances and some slight deformations in the connections.

Therefore the simulation results found by simulation are compatible with the experiments validating thus the simulation and the theoretical equations.

We also observe that in the function of the equations found theoretically, more the robot's vertical position decreases more the workspace increases. Since the legs can move even more in a near plane.

At a certain level, we cannot reach a few points of the workspace, it is limited by the workspace of point C, presented previously.

To increase the workspace, several parameters are involved:

- If we consider that the dimensions of the robot's platform are fixed, the lengths of the legs must be increased. But it is necessary to take into consideration the unreached positions which are previously shown in function of the dimensions L_2 and L_3.
- To increase the workspace, we have to reduce the contact distances with the ground, by bringing these distances closer to the dimensions of the robot (tending L to L_b and d to d_b).
- If $L - L_b = d - d_b$ the maximum displacements along the $\vec{x}$ and $\vec{y}$ axes are equals.
- To obtain a displacement along the $\vec{x}$ axis, greater than that along the $\vec{y}$ axis, $(L - L_b)$ must be less than $(d - d_b)$, which means that the angles of legs 1, 3, 4 and 6 respectively around the points D_1, D_3, D_4 and D_6 must not exceed 45°, with respect to the $\vec{y}$ axis.

8. CONCLUSION

The workspace of the hexapod robot is elaborated by a geometric approach considering a variety of dimensions and the contact distances of the robot. The versatility and the efficiency of workspace is made possible with GUI interface developed under SolidWorks platform.

The WorkPlane is also determined in a horizontal plane located at a desired height introduced on the GUI interface. It can also be defined in a vertical plane located at a desired distance. Therefore, all the reached positions of the robot will be known, in particular the limit positions. Thus we can optimize the hexapod robot structure based on its workspace.

The results are theoretically demonstrated and validated experimentally on a hexapod robot produced in the laboratory. Future works would be done to enhance the performances of the hexapod robot in terms of stability and mobility by exploring this geometrical approach.

REFERENCES

[1] E.G. Szadeczky Kardoss, Z. Gyenes, "Velocity obstacles for car-like mobile robots: Determination of colliding velocity and curvature pairs", Adv. Sci. Technol. Eng. Syst. J, vol. 3, no. 1, pp. 225-233, Jan. 2018.

[2] V.S. Bochkov, L.Yu. Kataeva, I.E. Belotserkovskaya, M.N. Ilicheva, "Prototype of forest fire suppression robotics system based on exclusionof flame

configuration frommonocular video sequence", ARPN Journal of Engineering and Applied Sciences, vol. 14, no. 9, pp. 1719-1730, May 2019.
[3] G. Scott, A. Ellery, "Using Bekker Theory as the Primary Performance Metric for Measuring the Benefits of Legged Locomotion over Traditional Wheeled Vehicles for Planetary Robotic Explorers", Space 2005, Long Beach, California, Aug. 2005.
[4] F. Zha, C. Chen, W. Guo, P. Zheng, J. Shi, "A free gait controller designed for a heavy load hexapod robot", Adv. Mech. Eng., vol. 11, no. 3, p. 168781401983836, Mar. 2019.
[5] D. Grzelczyk, J. Awrejcewicz, "On the Controlling of Multi-Legged Walking Robots on Stable and Unstable Ground", Dynamical Systems Theory, IntechOpen, 2020.
[6] J. Faigl, P. Cizek, "Adaptive locomotion control of hexapod walking robot for traversing rough terrains with position feedback only", Robot. Auton. Syst., vol. 116, pp. 136-147, Jun. 2019.
[7] E.H. Hasnaa, M. Bennani, "Robust control of an hexapod robot in lifting mode", International Conference on Electrical and Information Technologies (ICEIT), Rabat, Morocco, pp. 1-6, Mar. 2020.
[8] J. Sun, J. Ren, Y. Jin, B. Wang, D. Chen, "Hexapod robot kinematics modeling and tripod gait design based on the foot end trajectory", IEEE International Conference on Robotics and Biomimetics (ROBIO), Macau, pp. 2611-2616, Dec. 2017.
[9] R. Rodriguez, A. Fernando, M. Angel, A. Leiva, L.F. Ortiz, "Kinematic modelling of a robotic arm manipulatorusing matlab", ARPN Journal of Engineering and Applied Sciences, vol. 12, no. 7, pp. 2037- 2045, April 2017.
[10] J. Gabriel, O. Andres, J. Luis, R. Rodriguez, "Kinematic, dynamic modeling and design of a p-d controller for a four-degree-of-freedomrobot", ARPN Journal of Engineering and Applied Sciences, vol. 14, no. 5, pp. 1033-1042, March 2019.
[11] K. Nasir, R.L.A. Shauri, N.M. Salleh, N.H. Remeli, "Kinematic modelling for pid position control ofa new three-fingered robotic hand", ARPN Journal of Engineering and Applied Sciences, vol. 14, no. 2, pp. 335-343, January 2019.
[12] X.Y. Castro, E. C. Castaneda, "Statically stable adaptability strategies to change of terrain for a 6-limbed walking robot", Rev. Iberoam. Automatic and Informatics Ind., Dec. 2018.
[13] E.H. Hasnaa, M. Bennani, "Planning tripod gait of an hexapod robot", The 14th International Multi-Conference on Systems, Signals & Devices (SSD), Marrakech, pp. 163-168, Mar. 2017.
[14] M. Agheli, S.S. Nestinger,"Study of the Foot Force Stability Margin for multi-legged/wheeled robots under dynamic situations", The 8th IEEE/ASME International Conference on Mechatronic and Embedded Systems and Applications, Suzhou, China, pp. 99-104, Jul. 2012.
[15] A.Y.B. Hashim, S.H. Kamsani, M.M. Ali, S. Shamsuddin, A.Z. Shukor, "Simulation and Reproduction of a Manipulator According to Classical Arm Representation and Trajectory Planning", Adv. Sci. Technol. Eng. Syst. J., vol. 4, no. 6, pp. 158-162, 2019.
[16] X.Y. Sandoval Castro, M. Garcia Murillo, L.A. Perez Resendiz, E. Castillo Castaneda, "Kinematics of Hex-Piderix - A Six-Legged Robot - Using Screw Theory", International Journal of Advanced Robotic Systems, Vol. 10, p. 8, 2013.
[17] A. Jahi, I. Iskender, "Design and performance analysis of a three winding transformer used in solar system", International Journal on Technical and Physical Problems of Engineering (IJTPE), Issue 46, Vol. 13, No. 1, pp. 38-45, March 2021.
[18] F.Z. Derias, M. Mekakia, M.Z. Lounis "Quantitative and Qualitative Characterization of Municipal Solid Waste in Western Algeria: Impact of Population Growth", International Journal on Technical and Physical Problems of Engineering (IJTPE), Issue 45, Vol. 12, No. 4, pp. 28-35, December 2020.
[19] A. Lakhdar, A. Moumen, K. Mansouri, "Study of the mechanical behavior of bio loaded flexible pvc by coconut and horn fibers subjected to aging", International Journal on Technical and Physical Problems of Engineering (IJTPE), Issue 46, Vol. 13, No. 1, pp. 75-80, March 2021.
[20] W. Gouda, R.J.B. Chikha, "NAO Humanoid Robot Obstacle Avoidance Using Monocular Camera", Adv. Sci. Technol. Eng. Syst. J., vol. 5, no. 1, pp. 274-284, Feb. 2020.
[21] M. Atify, M. Bennani, A. Abouabdellah, "Propelling motion modeling of an Hexapod robot", The 1st International Conference on Smart Systems and Data Science (ICSSD), p. 5, Oct. 2019.
[22] C. Gosselin, "Determination of the Workspace of 6-DOF Parallel Manipulators", J. Mech. Des., vol. 112, no. 3, pp. 331-336, Sep. 1990.
[23] A. Cirillo, P. Cirillo, G. De Maria, A. Marino, C. Natale, S. Pirozzi, "Optimal custom design of both symmetric and unsymmetrical hexapod robots for aeronautics applications", Robot. Comput.-Integr. Manuf., vol. 44, pp. 1-16, Apr. 2017.
[24] Z.G. Yang, M.L. Shao, D.I. Shin, "Kinematic Optimization of Parallel Manipulators with a Desired Workspace", Appl. Mech. Mater., vol. 752-753, pp. 973-979, Apr. 2015.
[25] M. Agheli, S.S. Nestinger, "Comprehensive closed-form solution for the reachable workspace of 2-RPR planar parallel mechanisms", Mech. Mach. Theory, vol. 74, pp. 102-116, Apr. 2014.
[26] D. Chablat, L. Baron, R. Jha, "Kinematics and Workspace Analysis of a 3PPPS Parallel Robot With U-Shaped Base", Vol. 5B: 41st Mechanisms and Robotics Conference, Cleveland, Ohio, USA, p. V05BT08A065, Aug. 2017.
[27] M.O. Tokhi, G.S. Virk,"Advances in Cooperative Robotics", The 19th International Conference on Clawar 2nd World Scientific, 2016.
[28] M.U. Atique, R.I. Sarker, A.R. Ahad, "Development of an 8DOF quadruped robot and implementation of Inverse Kinematics using Denavit-Hartenberg

convention", Heliyon, vol. 4, no. 12, p. e01053, Dec. 2018.
[29] G. Wang, L. Ding, H. Gao, Z. Deng, Z. Liu, H. Yu, "Minimizing the Energy Consumption for a Hexapod Robot Based on Optimal Force Distribution", IEEE Access, vol. 8, pp. 5393-5406, 2020
[30] K. Xu, X. Ding, "Typical gait analysis of a six-legged robot in the context of metamorphic mechanism theory", Chin. J. Mech. Eng., vol. 26, no. 4, pp. 771-783, Jul. 2013.

BIOGRAPHIES

Mohamed Atify was born in Boulemane, Morocco in 1968. He received the mechanical aggregation from technical school (ENSET), Rabat, Morocco in 1998, and the master in mechanical engineering from technical school from University Mohammed V, Rabat, Morocco in 2016. He is currently working toward his Ph.D. in robotics, at the laboratory of systems engineering in Ibn Tofail University, Kenitra, Morocco. His research is focused on modeling, simulation and control of hexapod robots.

Mohammed Bennani is professor in Robotics and Control of dynamical systems at the ENSET engineering school, University Mohammed V, Rabat, Morocco. He received Ph.D. degree from EMI Rabat School, Morocco in 1997, and Master degree in Robotics from University of Montpellier, France in 1990. His research interests are modeling and control in robotics and motion and stability of celestial objects.

Abdellah Abouabdellah was born in Roummani, Morocco in 1968. He received Ph.D. degree in Science-Applied from Mohammed V University, Rabat, Morocco in 2010. He is a member of the energy team intelligent, electrical, industrial, attached to laboratory Systems Engineering at the University IbnTofail, Kenitra, Morocco. Currently, he is professor research at the National School of Applied Sciences, Kenitra, Morocco. He is also coordinator of the engineering sector in industrial and logistics engineering. He is the author, co-author of several articles in journals, national and international conferences. His research is the modeling of business processes, predictions systems and logistics.